Original Article
Journal of Biosystems Engineering
J. of Biosystems Eng. 40(4):305-313. (2015. 12)
http://dx.doi.org/10.5307/JBE.2015.40.4.305
eISSN : 2234-1862
pISSN : 1738-1266

# Fatigue Life Prediction of Crank-type Rotavator

**Dae-Chun Kim[1], Young-Jun Park[2]*, Geun-Ho Lee[2]**

[1]*R&D Institute, Tongyang Moolsan, Gongju, Chungcheongnam-do, Korea*
[2]*Department of System Reliability, Korea Institute of Machinery and Materials, Daejeon, Korea*

Received: September 22nd, 2015; Revised: November 16th, 2015; Accepted: November 26th, 2015

## Abstract

**Purpose:** This study was performed to predict the fatigue life of a crank-type rotavator operated in domestic soil conditions using Recurdyn®, a dynamic analysis program. **Methods:** Torque on the PTO shaft was measured using experiments conducted on the uplands and paddy fields in Korea. On the basis of the experimental and analytical results, the fatigue life of the crank-type rotavator was predicted by constructing an S-N curve according to the GL (Germanischer Lloyd Wind Energie GmbH) guideline. **Results:** The torques experienced by the PTO shaft in the paddy soil and the uplands were in the range of 472~797 N·m and 313~430 N·m, respectively, for every condition. In case of load condition, the peak torques (846 N·m, 770 N·m) were applied for severe conditions, resulting in a maximum (von Mises) stress of 75 MPa at the crank arm. The fatigue life of the crank-type rotavator was predicted to be 1,167 h that satisfies the target value of 1,110 h, by substituting the analysis results into an S-N curve of crank arm. **Conclusions:** The fatigue life of the crank-type rotavator was within the target life for the studied soil conditions; however, further field experiments for various soil conditions would be required to verify the prediction results.

**Keywords:** Crank-type rotavator, Fatigue life, GL guideline, S-N curve

## Introduction

Tillage operation at depths greater than 200 mm is very effective in improving the physical properties of soil (Varsa et al., 1997; Kim et al., 2001; Yoo et al., 2006). In Korea, plowing and/or plough tillage operation is followed by a rotavator operation as an in-depth operation. However, it is not feasible to perform in-depth subsoil tillage operation because most rotavators in Korea are rotary-type rotavators (Han et al., 1999). In the case of a rotary-type rotavator, there is widespread abrasion and breakage of the rotary blade because of the continuous rotation of the C- or L-type tillage blade in the soil. In addition, many tillage blades attached to one flange have the same operation section, which is not a suitable configuration for in-depth tillage operation because of the large traction resistance (Celik and Altikat, 2008) of the short tilling pitch. Therefore, a subsoil-type rotavator that allows for in-depth tillage operation with one tillage operation for subsoil tillage is required and economically favorable.

In Europe, including Italy, crank-type rotavators, which enable in-depth tillage operations up to depths of 300~400 mm in one tillage operation, and have one operation section for one tillage blade with a shovel-shaped blade, are widely used. In the case of a crank-type rotavator, a tillage blade operates at the same operation section. Compared to a rotary-type rotavator, the crank-type rotavator has a longer tilling pitch and shorter traction resistance. Moreover, the crank-type rotavator is also safe from abrasion and breakage of the tillage blades (NIAE, 2004) caused by stones or foreign substances because of the shoveling style of cultivating, and the crank-type rotavator enables in-depth tillage operation, regardless of the plough operation and rotavator operation. The soil is cultivated using an aggregated structure, and

***Corresponding author:** Young-Jun Park
**Tel:** +82-42-868-7994; **Fax:** +82-42-868-7477
**E-mail:** yjpark77@kimm.re.kr

therefore enables the creation of a favorable field environment for crop growth by increasing the water content in the soil stratum (Canarache, 1991; Pipitone et al., 2011).

In Korea, rotavator operation comprises 45% of the entire farm work cycle, and the power consumed by the tractor is the largest part, which mainly uses a rotary-type rotavator (Kim et al., 2011). Therefore, some studies were carried out with respect to the cultivation characteristics, although there is limited research on the use of crank-type rotavators (Nam et al., 2012). A crank-type rotavator is subjected to repeated loads during the cultivating operation due to its geometric structure. The repeated loads cause fatigue failure of the crank-type rotavator and result in a reduction in the productivity of the rotavator. Therefore, the study of the fatigue life with respect to the repeated loads should be performed in advance at the beginning of development in order to develop a crank-type rotavator that is suitable for domestic soil conditions.

Therefore, the objective of this study was to predict the fatigue life of a crank-type rotavator by fitting the stress values, obtained from simulations conducted using a commercial dynamic analysis program and measured using experiments, into an S-N curve.

## Materials and Methods

### Prototype rotavator and tractor

A crank-type prototype rotavator used in this study is shown in Figure 1. The specifications of the rotavator, requiring 45 kW power, are presented in Table 1.

The tractor used during rotavator operation had an output power of 48 kW, a nominal engine speed of 2,200 rpm, and 48 gear steps. The PTO has two gear steps, and its rotation speed is 550 rpm in the 1st gear and 733 rpm in the 2nd gear. Its specifications are presented in Table 2.

**Table 1.** Specifications of the rotavator used in this study

| Item | Specification |
|---|---|
| Model/Country | Prototype/Korea |
| Rated power, kW | 45 |
| Weight, kN | 5.8 |
| Nominal rotavating width, mm | 1,800 |
| Nominal rotavating depth, mm | 300 |

**Table 2.** Specifications of the prime mover tractor used in this study

| Item | Specification |
|---|---|
| Model/Country | T623/Korea |
| Length/Width/Height, mm | 3,725 × 1,840 × 2,545 |
| Weight, N | 24,353 |
| Engine rated power, kW/speed, rpm | 48/2,200 |
| No. of PTO gears (speed, rpm) | 2 (550/733) |

### Measurement system

#### *Data acquisition system*

In order to measure the torque on the PTO shaft, a torque meter (TRE-100K, Korea) was attached to the tractor, and the sensor signals from the torque meter were measured using a data acquisition system installed in the rear of the driver's seat (Figure 2).

The data acquisition system (DEWE-3010, Austria) sampled at a rate of 100 kHz with a resolution of 16 bits using DEWESOFT V6.1 (DEWETRON, Austria). It i receives both digital and analog signals and has the embedded signal amplification and noise filtering functions that can eliminate noise caused by the vibrations generated during

**Figure 1.** Photographs of the rotavator.

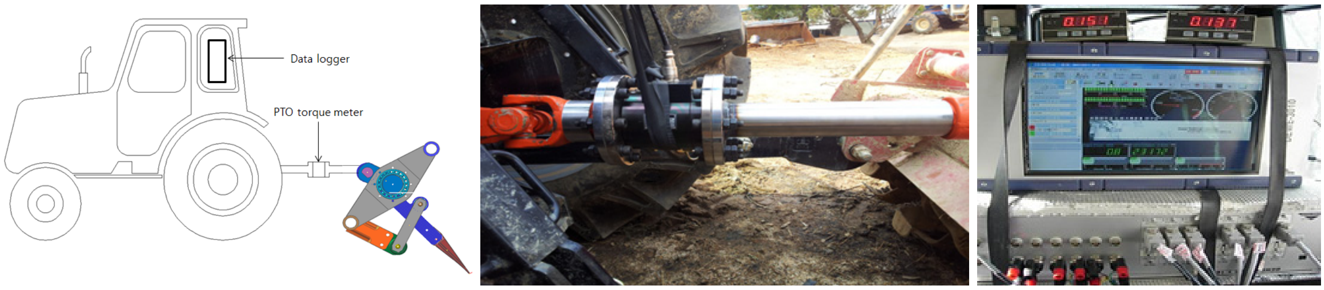


(a) Schematic diagram of measurement system (b) Torque meter installed at drive shaft (c) Data logger located in the cabin

**Figure 2.** Configuration of measurement system.

(a) Paddy field (b) Upland field

**Figure 3.** Photographs of the experimental plots.

**Table 3.** Soil properties of the experimental plots

| Site | Soil texture | Moisture content, %(d.b.) | Cone index by depth, kPa | | | | | |
|---|---|---|---|---|---|---|---|---|
| | | | Site | 5 cm | 10 cm | 15 cm | 20 cm | 25 cm |
| Paddy field | loamy sand | 29.7 | 1 | 175 | 351 | 496 | 596 | 2,317 |
| | | | 2 | 351 | 316 | 386 | 1,229 | 1,931 |
| | | 26.6 | 3 | 245 | 210 | 316 | 316 | 491 |
| | | | 4 | 140 | 210 | 245 | 351 | 2,317 |
| Upland field | loamy sand | 15.5 | 1 | 210 | 1,158 | 2,528 | 2,492 | 1,825 |
| | | | 2 | 140 | 667 | 1,580 | 1,896 | 2,176 |
| | | 14.2 | 3 | 70 | 1,580 | 2,106 | 2,071 | 1,755 |
| | | | 4 | 140 | 526 | 1,509 | 1,615 | 2,141 |

the field experiments and other sources.

## Field test

### *Test site description*

The field experiments were performed at a paddy field located in Sangwol-myun, Nonsan-si, Chungcheongnam-do and an upland field located in Baekgu-myun, Gimje-si, Jeollabuk-do, as shown in Figure 3. The soil texture and moisture content of experimental fields were measured using the USDA soil texture triangle obtained from two different randomly selected experimental soils. The soil strengths were measured at four randomly selected locations in the experimental field by using a cone penetrometer (SC900, Spectrum Technology, USA) with spacing of 5cm at depths of 0~25 cm.

The test results for the soil textures, moisture content, and soil strength are summarized in Table 3. The paddy soil consisted of 74% sand, 25.2% silt, and 0.8% clay, whereas the upland soil consisted of 70.4% sand, 28.7% silt, and 0.9% clay. Both soils contained loamy sand. The

**Table 4.** Gears for rotavator operation and corresponding nominal work speeds of the tractor

| Gear | Nominal work speed, km/h |
|---|---|
| L2 | 1.41 |
| L3 | 2.17 |
| L4 | 2.70 |
| M1 | 2.85 |
| PTO | Nominal rotating speed, rpm |
| 1 | (550/733) |

moisture content in the paddy soil was 29.7% and 26.6%, and those in upland soil were 15.5% and 14.2%. The strengths of the paddy and upland soils were in the range of 140~2,317 kPa and 70~2,528 kPa, respectively.

### *Work conditions*

In general, for the cultivating operation performed using a crank-type rotavator, a combination of gear L2 and PTO gear 1 is used. However, the experiment was performed with gears L2, L3, L4, and M1 to compare the load characteristics under various conditions, while the engine and the PTO were fixed at the nominal speed and 1st gear, respectively.

The operating distance for each operating condition was 15 m, and each operation was repeated twice. The operating conditions and their nominal speeds for each soil are listed in Table 4.

## Fatigue analysis

### *Modeling*

A complete and simplified 3D model of the crank-type rotavator are built as shown in Figure 4, and the materials of the model elements are listed in Table 5. The crank arm, blade frame, and rollers were modeled as flexible bodies that were expecting fatigue failure caused by the repeated load on the parts. However, the main frame and blades were modeled as rigid bodies because the main frame was not influenced by the load transferred from the cultivating operation, and the blades were generally influenced by friction.

### *Boundary conditions*

A commercial dynamic analysis program (Recurdyn V8R1, Functionbay, Korea) was used for analyzing the stress experienced by the crank-type rotavator. The constraint conditions were set considering the actual operation conditions of the rotavator, and the material properties (Figure 4b) of each part were the same as the actual parts. In addition, the operating speed of tractor for driving the

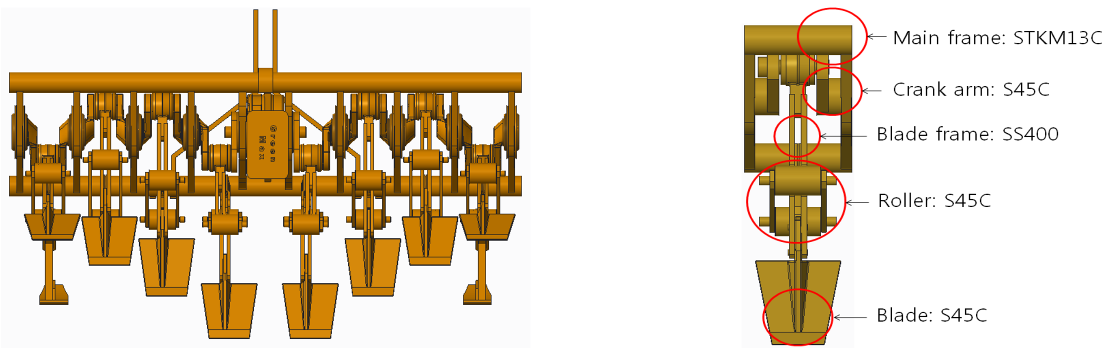


(a) Full model (b) Simplified model

**Figure 4.** Models of the rotavator with materials.

**Table 5.** Physical properties of the rotavator

| Title | Material | Young's modulus, GPa | Tensile strength, MPa | Yield strength, MPa |
|---|---|---|---|---|
| Main frame | STKM13C | 206 | 510 | 380 |
| Crank arm | S45C | 190–210 | 569 | 343 |
| Blade frame | SS400 | 190–210 | 400–510 | 205–245 |
| Roller | S45C (Quenching Tempering) | 190–210 | 686 | 490 |
| Blade | S45C | 190–210 | 569 | 343 |

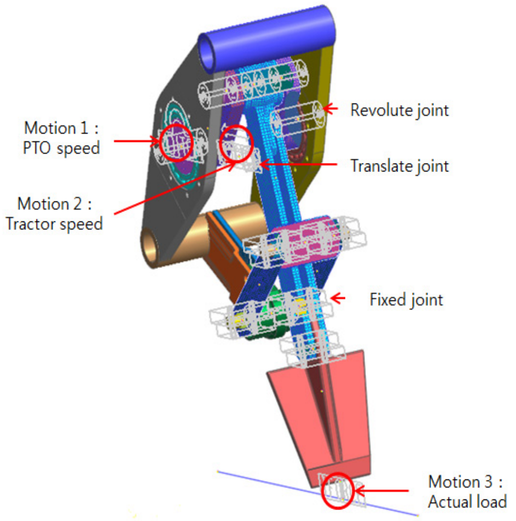


**Figure 5.** Joint configuration of the rotavator.

rotavator and the rotation speed of the tillage blades were applied to the analysis as additional parameters. The model and joint configuration for the dynamic analysis of the crank-type rotavator are shown in Figure 5.

## *Loading condition*

The load measurement results obtained from the experiments on actual soil were used as the loading conditions for dynamic analysis. Moreover, the peak torque profile acting on a tillage blade was extracted from the torque profile of PTO shaft obtained from an actual field test. Figures 6 and 7 show the measured torque profile of PTO shaft and the peak torque values that act on a tillage blade, respectively.

## *S-N curve*

The S-N curve was constructed based on the GL guideline (GL Guideline, 2010) by using tensile strength, yield strength, thickness, surface roughness of the material, grades of parts, constants and stress ratio for the material, and the test method. A synthetic S-N curve can be constructed as shown in Figure 8, using the input and resulting parameters from Table 6 and 7.

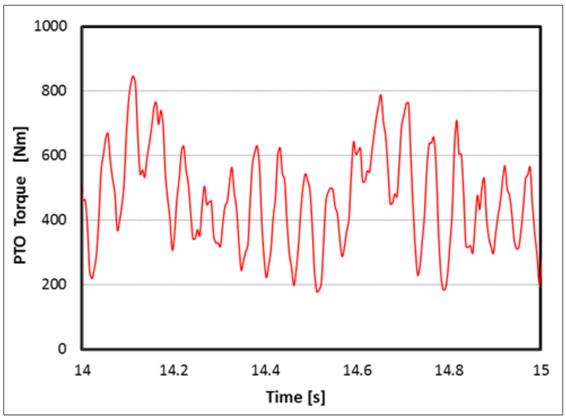


**Figure 6.** Measured torque profile on the PTO shaft.

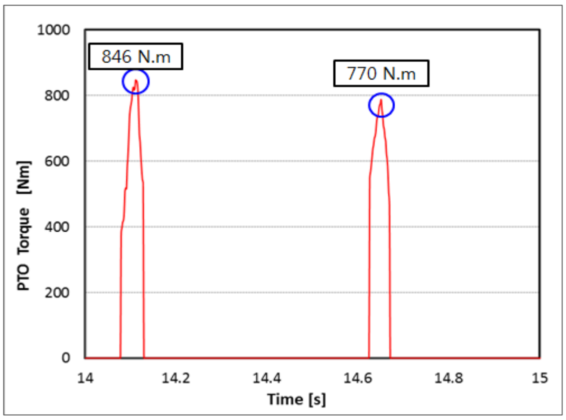


**Figure 7.** Extracted peak torque values.

**Table 6.** Input parameters for the calculation of the synthetic S-N curves

| Symbol | Meaning | Value | Units |
|---|---|---|---|
| $R_m$ | Tensile strength | 569 | N/mm² |
| $R_{p0.2}$ | Yield strength | 343 | N/mm² |
| R | Stress ratio | 0 | - |
| $\alpha_k$ | Stress concentration factor | 1 | - |
| n | Notch sensitivity caused by the stress gradient and localized plastic deformation at the notch base | 1 | - |
| $R_z$ | Surface roughness | 160 | μm |
| $\gamma_M$ | Partial safety factor for the material | 1.265 | - |
| j | Quality level for the component | 3 | - |
| $j_0$ | Constant for the material and test method | 0 | - |
| t | Wall thickness | 25 | mm |

**Table 7.** Resulting parameters defining the synthetic S-N curve

| Symbol | Meaning | Value | Units |
|---|---|---|---|
| $\Delta\sigma_1$ | Upgraded upper limit of the fatigue life line | 271 | N/mm² |
| $N_1$ | Number of load cycles at the upper fatigue limit | 177 | - |
| $\Delta\sigma_A^*$ | Upgraded stress range at the knee of the S-N curve | 88 | N/mm² |
| $N_D$ | Number of load cycles at the knee of the S-N curve | 2,370,371 | - |
| $m_1$ | Slope of the S-N curve for N1< N ≤ ND | 8.647 | - |
| $m_2$ | Slope of the S-N curve for N > ND | 15.934 | - |

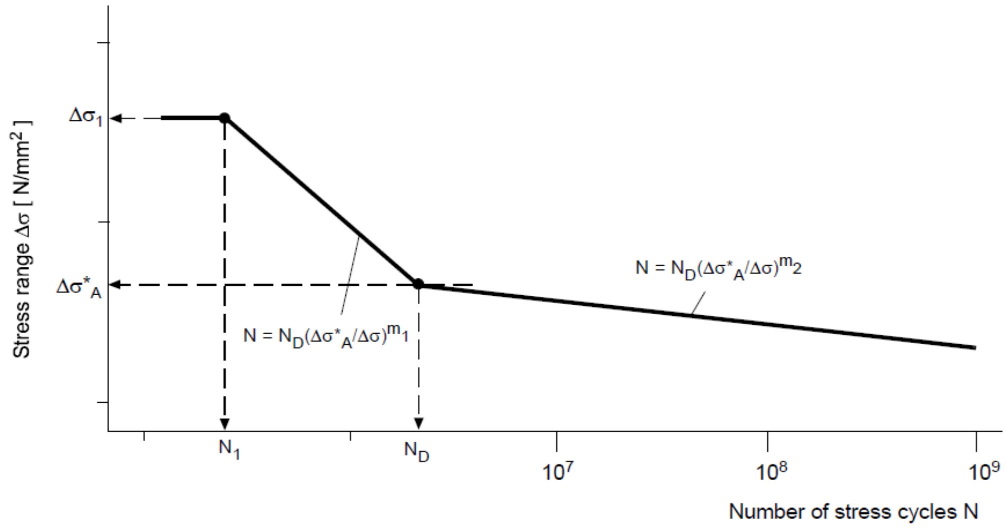


**Figure 8.** Graph of the synthetic S-N curve.

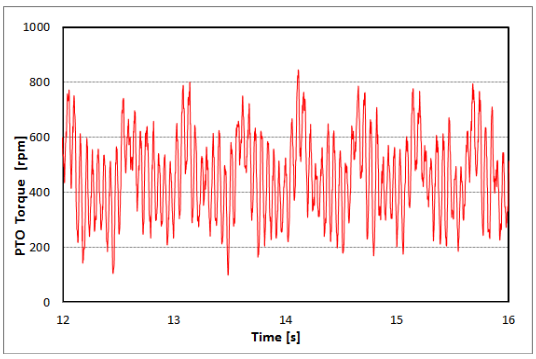


(a) Paddy field

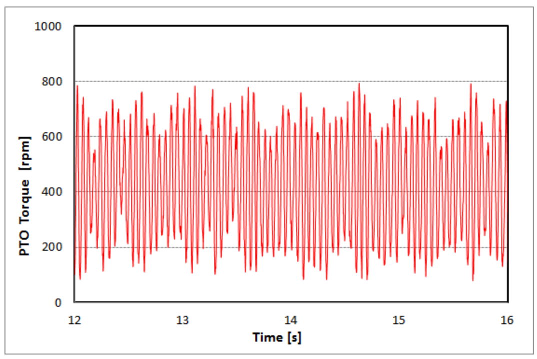


(b) Upland field

**Figure 9.** PTO torque measured with the torque meter.

# Results and Discussion

## PTO torque

The results of the torque measurement on the PTO shaft showed that the average torques in the upland and paddy fields were in the ranges of 313~430 N·m and 472~797 N·m, respectively. This result demonstrated that the torque in the paddy field was larger than that in the upland field for every driving condition (Choi and NahmGung, 2000) because the cultivation resistance is sufficiently large owing to the higher moisture content of the paddy field. During the cultivating operation, the torque transmitted to the PTO shaft is shown in Figure 9, and the average torques in both the paddy and upland fields are listed in Table 8.

**Table 8.** Comparison of the average PTO torques in the upland field and paddy field

| Gear Tractor/PTO | Upland field, N·m | | Paddy field, N·m | |
|---|---|---|---|---|
| | 1st | 2nd | 1st | 2nd |
| L2/PTO 1 | 430.09 | 362.47 | 567.21 | 796.97 |
| L3/PTO 1 | 408.09 | 352.17 | 631.08 | 748.65 |
| L4/PTO 1 | 363.47 | 337.13 | 537.31 | 650.92 |
| M1/PTO 1 | 322.25 | 313.37 | 472.34 | 613.32 |

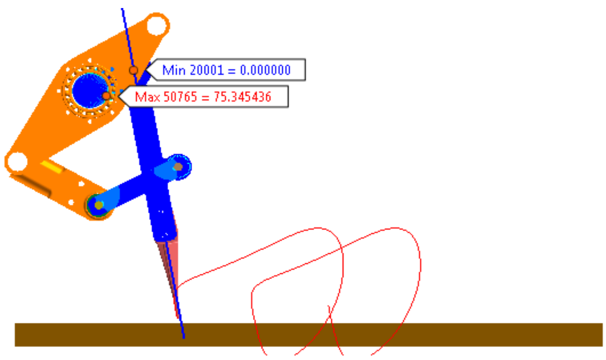


**Figure 10.** Image of the dynamic analysis.

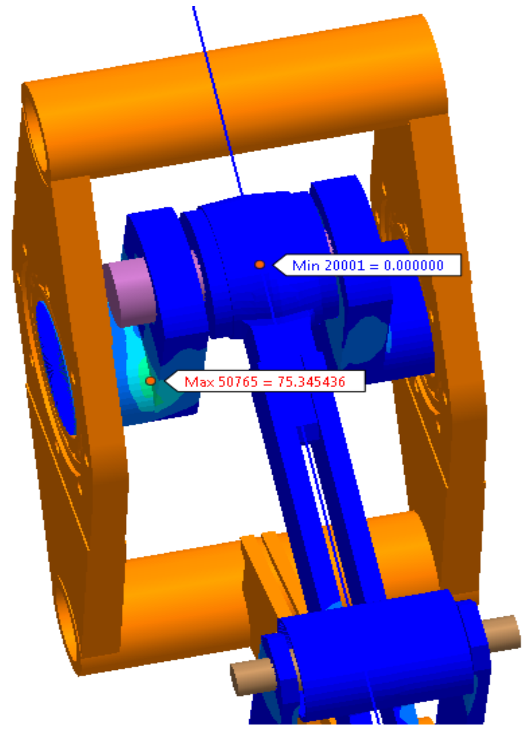


**Figure 11.** Position of maximum stress in the rotavator model.

## Dynamic stress analysis

Considering the actual operating conditions of the rotavator, a stress analysis was performed (Figure 10). The load acting on the ends of the tillage blades was calculated taking into account the gear ratio and the torque measured on the PTO shaft In order to perform a conservative analysis under severe conditions, severe load conditions were applied with the peak torque (846 N·m and 770 N·m, Figure 7) instead of the average torque. Based on the results of the stress analysis, it was found that the maximum von Mises stress of 75 MPa occurred at the crank arm, and the maximum stress and a graph of the maximum stress nodes are shown in Figures 11 and 12, respectively.

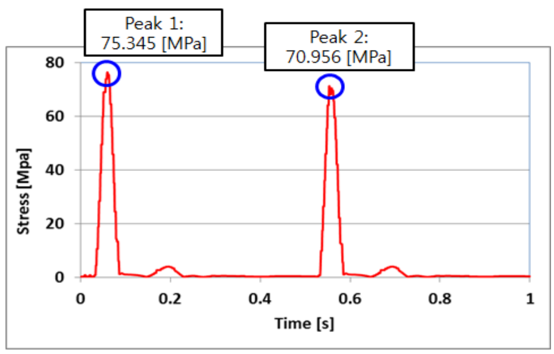


**Figure 12.** Graph of the maximum stress node.

## Fatigue life prediction

Figure 13 and Table 9 present the results for the predicted fatigue life using the S-N curve. The fatigue life obtained by applying the stress values of peaks 1 and 2 (75 MPa and 71 MPa, Figure 12) to the S-N curve correspond to $9.05 \times 10^6$ cycles and $1.50 \times 10^7$ cycles, respectively. In general, the target life of an agricultural machine is 10 years (Kim and Kang, 2009; Sim et al., 2011), and the annual usage time of a rotavator with a 37~58 kW tractor in Korea is 110 h (Kim et al., 2011). That is, the target life of the rotavator becomes 1,100 h, and this is converted to $1.07 \times 10^7$ cycles. Figure 12 shows the graph when a rotavator rotates twice, indicating two cycles, and the target life of peaks 1 and 2 is 550 h, resulting in $5.32 \times 10^6$ cycles. The fatigue damage for peaks 1 and 2 calculated using the obtained fatigue life are 58.9% and 35.4%, respectively and total damage is 94.3%. Therefore, the fatigue life of the crank-type rotavator was 1,167 h calculated for a target life of 1,100 h with a total damage of 94.3%, and it was within the target life for the studied soil conditions. However, further field experiments are required that consider various soil conditions to verify the fatigue life prediction results.

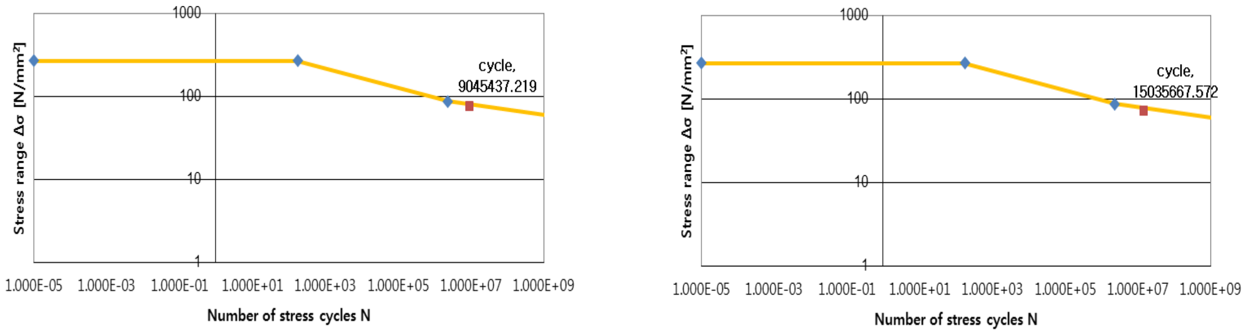


(a) Peak 1 (b) Peak 2

**Figure 13.** Application of S-N curve for the crank-type rotavator at peak 1 and peak 2.

**Table 9.** Results of fatigue life prediction

| No | Equivalent stress, MPa | Life with respect to the S-N curve, no. of cycles | Target life, no. of cycles | Damage, % | Total damage, % | Predicted life, hours |
|---|---|---|---|---|---|---|
| Peak 1 | 75 | 9.05x106 | 5.32x106 | 58.9 | 94.3 | 1,167 |
| Peak 2 | 71 | 1.50x107 | | 35.4 | | |

## Conclusions

This study was performed to predict the fatigue life of a crank-type rotavator operated under domestic soil conditions using a dynamic analysis program. The torque on the PTO shaft was measured during experimental tests conducted using rotavators on the uplands and paddy fields in Korea. On the basis of experimental and analytical results, the fatigue life of the crank-type rotavator was predicted by constructing an S-N curve based on the GL guideline. A summary of the results is as follows.

(1) The results of the torque measurements on the PTO shaft showed that the torques on the PTO shaft in paddy soil were in the range of 472~797 N·m, whereas the torques on the PTO shaft for the upland were in range of 313~430 N·m, for every condition.

(2) The peak torque values were used to predict the fatigue life of the rotavator under severe test conditions. The results of the field experiment showed that the torques on the PTO shaft were observed twice per second, and torques represented by peak 1 and 2 were 846 N·m and 770 N·m, respectively.

(3) The results of the dynamic analysis considering the peak torque and actual operating conditions showed that the maximum stress occurred at the crank arm, and the von Mises stresses were 75 MPa and 71 MPa for the peaks 1 and 2, respectively.

(4) The S-N curve was constructed according to the GL guideline, and the fatigue life of the rotavator was obtained by applying the stress values of peaks 1 and 2 (75 MPa and 71 MPa) to the S-N curve correspond to $9.05x10^6$ cycles and $1.50x10^7$ cycles, respectively. In addition, the fatigue damage was 58.9% and 35.4% for the peak 1 and peak 2, respectively, for a target life of 1,100 h.

(5) The fatigue life of the crank-type rotavator for the studied soil conditions was predicted to be 1,167 h, which satisfies the target value of 1,110 h. However, further field experiments for various soil conditions are required to verify the prediction results.

## Conflict of Interest

The authors have no conflicting financial or other interests.

## References

Canarache, A. 1991 Factors and indices regarding excessive compactness of agricultural soils. Soil and Tillage Research 19:145-164.
Celik., A. and S. Altikat. 2008. Geometrical analysis of the

effects of rotary tiller blade path on the distribution of soil slice size. American Society of Agricultural and Biological Engineers 24(4):409-413.

Choi, C. H. and M. J. NahmGung. 2000. Load measurement of tractor on field performance. In: *Proceedings of the KSAM 2000 Summer Conference* 25:29-34.

Germanischer Lloyd WindEnergieGmbH (GL). 2010. Guideline for the Certification of Wind Turbines. GL 2010.

Han, K. H., K. U. Kim and Y. G. Wu. 1999. Severeness of transmission loads of agricultural tractor for rotary operations in poorly drained paddy field. Journal of Biosystems Engineering 24(4):293-300.

Kim, D. C. and Y. S. Kang. 2009. Case study of accelerated life test method for agricultural tractor transmission. Journal of Biosystems Engineering 34(5):325-330.

Kim, L. Y., H. J. Cho, B. K. Hyun and W. P. Park. 2001. Effects of physical Improvement practices at plastic film house soil. Journal of Korea Society of Soil Science and Fertilizer 34(2):92-97.

Kim, Y. J., S. O. Chung, S. J. Park and C. H. Choi. 2011. Analysis of power requirement of agricultural tractor by major field operation. Journal of Biosystems Engineering 36(2):79-88.

Nam, J. S., D. S. Kang, Y. S. Kang, K. U. Kim and D. C. Kim. 2012. Comparison of work performance of crank-type and rotary-type rotavators in Korean farmland conditions. Journal of Biosystems Engineering 37(3):140-147.

NIAE. 2004. Experimental and research report. Suwon, Korea: National Institute of Agricultural Engineering.

Pipitone, F., P. Catania and M. Vallone. 2011. First results on the use of an innovative machine for soil tillage in terraces or steep sloped areas. Efficient and safe production processes in sustainable agriculture and forestry. In: *Proceedings of the XXXIV CIOSTA CIGR V Conference*.

RECURDYN V8R1 Program manual. 2012. FUNCTIONBAY.

Sim, K. J., W. Y. Cho and Y. J. Lee. 2011. Development on test specification of reliability of agricultural tractor. In: *Proceedings of the KSAE 2011 Fall Conference* 19(2):43-48.

Varsa, E. C., S. K. Chong, J. O. Aboaji, D. A. Farquhar and F. J. Olsen. 1997. Effect of deep tillage on soil physical characteristics and corn (*Zea mays* L.) root growth and production. Soil and Tillage Research 43:219-228.

Yoo, C. H., J. H. Ryu, C. H. Yang, T. K. Kim, S. W. Kang, J. D. Kim and K. Y. Jung. 2006. Influence of diagnostic fertilization and subsoil breaking on soil physico-chemical properties in direct seeding of rice on flooded paddy surface. Journal of Korean Society of Soil Science and Fertilizer 39(6):334-338.